



# Rifampin and ritonavir increase oral availability and elacridar enhances overall exposure and brain accumulation of the NTRK inhibitor larotrectinib

Yaogeng Wang<sup>a</sup>, Rolf W. Sparidans<sup>b</sup>, Jing Wang<sup>a</sup>, Wenlong Li<sup>a</sup>, Maria C. Lebre<sup>a</sup>,  
Jos H. Beijnen<sup>a,b,c</sup>, Alfred H. Schinkel<sup>a,\*</sup>

<sup>a</sup> The Netherlands Cancer Institute, Division of Pharmacology, Plesmanlaan 121, 1066 CX Amsterdam, the Netherlands

<sup>b</sup> Utrecht University, Faculty of Science, Department of Pharmaceutical Sciences, Division of Pharmacology, Universiteitsweg 99, 3584 CG Utrecht, the Netherlands

<sup>c</sup> The Netherlands Cancer Institute, Department of Pharmacy & Pharmacology, Plesmanlaan 121, 1066 CX Amsterdam, the Netherlands

## ARTICLE INFO

### Keywords:

Larotrectinib

ABCB1

OATP1A

Elacridar

Rifampin

Ritonavir

Cytochrome P450-3A

Oral availability

## ABSTRACT

**Introduction:** Larotrectinib is an FDA-approved oral small-molecule inhibitor for neurotrophic tropomyosin receptor kinase (NTRK) fusion-positive cancer treatment. Here larotrectinib pharmacokinetic behavior upon co-administration with prototypical inhibitors of the efflux transporters ABCB1/ABCG2 (elacridar), the SLCO1A/1B (OATP1A/1B) uptake transporters (rifampin), and the drug-metabolizing enzyme CYP3A (ritonavir), respectively, was investigated.

**Methods:** Inhibitors were orally administered prior to oral larotrectinib (10 mg/kg) to relevant genetically modified mouse models. Larotrectinib plasma and tissue homogenate concentrations were measured by a liquid chromatography-tandem mass spectrometric assay.

**Results:** Elacridar increased oral availability (2.7-fold) and markedly improved brain-to-plasma ratios (5.0-fold) of larotrectinib in wild-type mice. Mouse (m)Oatp1a/1b but not hepatic transgenic human (h)OATP1B1 or –1B3 restricted larotrectinib oral availability and affected its tissue distribution. Rifampin enhanced larotrectinib oral availability not only in wild-type mice (1.9-fold), but surprisingly also in *Slco1a/1b*<sup>−/−</sup> mice (1.7-fold). Similarly, ritonavir increased the larotrectinib plasma exposure in both wild-type (1.5-fold) and *Cyp3a*<sup>−/−</sup> mice (1.7-fold). Intriguingly, both rifampin and ritonavir decreased liver and/or intestinal larotrectinib levels in all related experimental groups, suggesting additional inhibition of enterohepatic Abcb1a/1b activity.

**Conclusions:** Elacridar enhances both larotrectinib plasma and tissue exposure and especially relative brain penetration, which might be therapeutically relevant. Hepatic mOatp1a/1b but not hOATP1B1 or –1B3 transported larotrectinib. Additionally, rifampin enhances larotrectinib systemic exposure, most likely by inhibiting mOatp1a/1b, but probably also hepatic and/or intestinal mAbcb1. Similar to rifampin, dual-inhibition functions of ritonavir affecting both CYP3A enzymes and enterohepatic Abcb1 transporters enhanced larotrectinib oral availability. The obtained insights may be used to further optimize the clinical-therapeutic application of larotrectinib.

## 1. Introduction

The Neurotrophic Tropomyosin Receptor Kinase (NTRK) family

contains three nerve growth factor receptor genes, NTRK1, NTRK2 and NTRK3, which encode the single-transmembrane receptor tyrosine kinases TRK A, B, and C, respectively [1]. These receptors are essential for

**Abbreviations:** ABC, ATP-binding cassette; ABCB1, ATP-binding cassette sub-family B member 1; ABCG2, ATP-binding cassette super-family G member 2; BBB, Blood-brain-barrier; BTB, Blood-testis-barrier; CYP, Cytochrome P450; Cyp3aXAV, Cyp3a knockout mice with specific expression of human CYP3A4 in liver and intestine; DDI, drug-drug interaction; LC-MS/MS, liquid chromatography coupled with tandem mass spectrometry; NTRK, Neurotrophic tropomyosin receptor kinase; OATP, Organic anion-transporting polypeptide; P-gp, P-glycoprotein; SLCO, OATP solute carrier family; SI + SIC, Small intestine together with small intestinal contents; TKI, tyrosine kinase inhibitor.

\* Corresponding author at: Division of Pharmacology, The Netherlands Cancer Institute, Plesmanlaan 121, 1066 CX Amsterdam, The Netherlands.

E-mail address: [a.schinkel@nki.nl](mailto:a.schinkel@nki.nl) (A.H. Schinkel).

<https://doi.org/10.1016/j.ejpb.2021.12.007>

Received 2 September 2021; Received in revised form 13 December 2021; Accepted 16 December 2021

Available online 21 December 2021

0939-6411/© 2021 Elsevier B.V. All rights reserved.

proliferation and survival of neurons. However, albeit infrequently, oncogenic fusions among the NTRK genes may occur in a variety of adult malignancies and pediatric cancers, including glioblastoma, non-small cell lung cancer (NSCLC), and colorectal cancer [2–4]. In November 2018, the FDA approved a first selective pan-TRK inhibitor, larotrectinib (Vitrakvi, LOXO-101, Supplemental Fig. 1) [5], which could induce marked tumor shrinkage in patients with NTRK-rearranged cancers.

As two important members of the ABC drug efflux transporters, P-glycoprotein (P-gp; ABCB1) and breast cancer resistance protein (BCRP; ABCG2) are highly expressed in the blood-facing luminal membrane of the physiological barriers protecting pharmacological sanctuary compartments, including blood–brain barrier (BBB) and blood–testis barrier (BTB), and in the apical membranes of epithelial cells in organs that are responsible for drug absorption and elimination, such as enterocytes and hepatocytes [6]. Organic anion-transporting polypeptides (SLCO; OATPs) are expressed mainly in liver, kidney and small intestine, where they mediate the tissue uptake of many endogenous and exogenous compounds. Thus, these transmembrane transporters could influence the distribution of molecules between blood and tissues.

It has previously been demonstrated that mAbcb1a/1b and mAbcg2 together can markedly limit larotrectinib oral availability and brain accumulation in mice by 2.1- and 10.4-fold, respectively. Interestingly, mSlco1a/1b (Oatp1a/1b) also restricted larotrectinib oral availability (by 3.8-fold), apparently by mediating substantial uptake into the liver [7]. *In vitro* uptake assays suggested that larotrectinib is very likely a substrate of human OATP1A2 (SLCO1A2), but not of human OATP1B1 (SLCO1B1) or –1B3. However, OATP-mediated uptake of certain substrates can be cell-type dependent for as yet unknown reasons [8], so a negative result does not necessarily mean that a substrate cannot be transported under all circumstances. For this reason *in vivo* studies and vigilance in recognizing possible OATP-mediated drug–drug interactions during the clinical application of larotrectinib are still advisable.

The multidrug-metabolizing Cytochrome P450 3A (CYP3A) enzyme complex is responsible for most phase I drug metabolism. CYP3A4 is the most highly expressed CYP enzyme in human liver, one of the main detoxification organs, but also in the small intestine. It therefore profoundly contributes to the oxidative metabolism of nearly half of the drugs currently in clinical use, resulting in drug inactivation or sometimes also activation [9,10]. Larotrectinib was demonstrated to be an excellent *in vivo* substrate of CYP3A enzymes in our previous study [7]. However, many ABCB1 and/or ABCG2 substrates are also substrates and/or inhibitors for CYP3A, and it has been hypothesized that the combined activity of drug efflux transporters and CYP3A results in efficient first-pass metabolism of orally administered drugs [11–15]. As larotrectinib is an excellent substrate of ABC efflux and OATP1 uptake transporters, as well as CYP3A enzymes, these properties may complicate larotrectinib pharmacokinetics: activity variation through gene polymorphisms or exogenous factors such as inhibitors or inducers of transporters and metabolizing enzymes could all affect larotrectinib behavior.

Drug–drug interactions (DDIs) may cause changes in the absorption, distribution, metabolism and excretion (ADME) of a drug and can result in variable drug exposure leading to potential toxicities or altered efficacy. This includes interfering with drug transporters such as ABCB1 and ABCG2, or the OATPs, or interfering with drug-metabolizing enzymes such as CYP3A, or even both. Co-administration of elacridar, a dual inhibitor of ABCB1 and ABCG2, could improve both oral exposure and brain penetration of several tyrosine kinase inhibitors (TKIs), such as sorafenib, crizotinib, vemurafenib, ribociclib, and others [16–19]. Besides, OATP uptake transporters could be inhibited by the prototypical Oatp1a/1b inhibitor rifampin, which leads to reduced uptake of many endogenous molecules and drugs, like statins [20]. Of note, rifampin can not only inhibit OATPs, but also ABCB1 to some extent. Rifampin further displays a kind of dual function, including acute inhibition of ABCB1 and OATPs, but also chronic gene induction of ABCB1 and CYP3A [21]. With respect to CYP3A inhibitors, the HIV protease inhibitor ritonavir can

efficiently inhibit CYP3A activity and thus substantially boost systemic exposure of many drugs, such as docetaxel, paclitaxel, and lopinavir [22,23]. However, like rifampin, ritonavir can also inhibit ABCB1 [24,25].

In the present study, the first aim was to investigate whether larotrectinib is a substrate of human OATP1B1 and OATP1B3 *in vivo* using human OATP transgenic mice. Larotrectinib can be transported by ABCB1, ABCG2 and OATP1A, and it can also be metabolized by CYP3A. Thus, potentially genetic polymorphisms and exogenous inhibitors/inducers affecting all these systems may influence the pharmacokinetics, and hence the safety and efficacy profiles of larotrectinib. Therefore, further exploration was performed to see whether substantial alterations in oral availability and tissue distribution, including brain penetration, could be induced by inhibition of ABCB1/ABCG2, OATP1A/1B, or CYP3A using oral co-administration of elacridar, rifampin, or ritonavir, respectively.

## 2. Materials and methods

### 2.1. Chemicals

Larotrectinib was purchased from Carbosynth (Oxford, UK). Ritonavir and elacridar HCl were obtained from Sequoia Research Products (Pangbourne, UK). Rifampin was from Sigma-Aldrich (Steinheim, Germany). Bovine Serum Albumin (BSA) Fraction V was obtained from Roche Diagnostics GmbH (Mannheim, Germany). Glucose water 5% w/v was from B. Braun Medical Supplies (Melsungen, Germany). Isoflurane was purchased from Pharmachemie (Haarlem, The Netherlands), heparin lithium (5000 IU ml<sup>−1</sup>) was from Leo Pharma (Breda, The Netherlands). All chemicals used in the larotrectinib LC-MS/MS assay were described before [26]. All other chemicals and reagents were obtained from Sigma-Aldrich (Steinheim, Germany).

### 2.2. Animals

Wild-type, Abcb1a/1b;Abcg2<sup>−/−</sup> [27], Slco1a/1b<sup>−/−</sup> [28], Slco1B1 [29], Slco1B3 [30], Cyp3a<sup>−/−</sup> [9] and Cyp3aXAV [9] male mice, all of a > 99% FVB genetic background, were used between 9 and 16 weeks of age. All the mouse strains were established and characterized before. Animals were kept in an SPF animal facility, in a temperature-controlled environment with 12-h light and 12-h dark cycle. They received a standard diet (Transbreed, SDS Diets, Technilab – BMI, Someren, The Netherlands) and acidified water *ad libitum*. Mice were housed and handled according to institutional guidelines complying with Dutch and EU legislation. In this study, only male mice were randomly allocated for experiments. Because the main read-out of these experiments was objective (larotrectinib plasma and tissue concentrations as measured by LC-MS/MS), no blinding method was applied. All experimental animal protocols were evaluated and approved by the institutional animal care and use committee and experimental procedures were optimized to follow the 3R principles (replacement, refinement, reduction).

### 2.3. Drug solutions

For oral administration, larotrectinib was dissolved in dimethyl sulfoxide (DMSO) at a concentration of 50 mg/ml and further diluted with 5% (w/v) glucose in water to yield a concentration of 1.0 mg/ml. Final concentrations for DMSO and glucose in the dosing solution were 2% (v/v) and 4.75% (w/v), respectively. Elacridar hydrochloride was dissolved in DMSO (106 mg/ml) in order to get 100 mg elacridar base per ml DMSO. The stock solution was further diluted with a mixture of polysorbate 20, ethanol and water [20:13:67, (v/v/v)] to yield a concentration of 10 mg/ml elacridar. Rifampin was first dissolved in DMSO to yield a 100 mg/ml stock solution, and further diluted with polysorbate 20, absolute ethanol and 5% glucose water, to obtain a final working solution of 10 mg/ml [in DMSO: polysorbate 20: ethanol: 5%

glucose water = 10:15:15:60, (v/v/v/v)]. For the ritonavir boosting experiment, 30 mg/ml ritonavir was dissolved in polysorbate 20/ethanol (1:1, v/v) and stored at  $-30^{\circ}\text{C}$ . This was then further diluted with 5 parts of water (1:5, v/v) to obtain a 5 mg/ml working solution for administration. All dosing solutions were prepared freshly on the day of experiment.

#### 2.4. Larotrectinib administration schedules with targeted inhibitors

To minimize variation in absorption upon oral administration, all the mice were fasted for 3 h before any inhibitors and larotrectinib were administered orally. Larotrectinib was administered at a dose of 10 mg/kg, while elacridar and rifampin were both administered at a dose of 100 mg/kg. For ritonavir boosting, 15 mg/kg of larotrectinib was used after 50 mg/kg ritonavir was administered. All the drug working solutions were administered by gavage using a blunt-ended needle, applying 10  $\mu\text{L}$ /g of body weight. Elacridar was orally administered 3 h prior to oral larotrectinib administration in wild-type and *Abcb1a/1b;Abcg2*<sup>-/-</sup> mice, as its plasma  $C_{\text{max}}$  is known to occur around 4 h, thus maximizing its capacity to inhibit transporters in the BBB. In contrast to elacridar, ritonavir and rifampin were expected to exert their primary inhibitory functions in intestine and liver (and not the BBB). As intestine and liver are usually maximally exposed shortly after oral administration of drugs, ritonavir and rifampin were administered 15 min before larotrectinib. Thus, for the rifampin inhibition experiments, rifampin was administered first, and larotrectinib was administered orally 15 min later in wild-type, *Slco1a/1b*<sup>-/-</sup>, *Slco1B1* and *Slco1B3* mice. Similarly, for ritonavir inhibition experiments, ritonavir was administered orally 15 min prior to oral larotrectinib in wild-type, *Cyp3a*<sup>-/-</sup> and *Cyp3aXAV* mice.

#### 2.5. Plasma and organ pharmacokinetics of larotrectinib in mice

For all the inhibition experiments, approximately 50  $\mu\text{L}$  tail vein blood samples were collected at 7.5 min (0.125 h), 15 min (0.25 h), 30 min (0.5 h) and 45 min (0.75 h) after oral larotrectinib administration, using microvettes containing dipotassium-EDTA. At the last time point (1 h), mice were anesthetized with 5% isoflurane and blood was collected by cardiac puncture. Blood samples were collected in Eppendorf tubes containing heparin as an anticoagulant. The mice were then sacrificed by cervical dislocation and brain, liver, kidney, small intestine together with small intestine contents (SI + SIC) and testis were rapidly removed. Plasma was isolated from the blood by centrifugation at  $9,000 \times g$  for 6 min at  $4^{\circ}\text{C}$ , and the plasma fraction was collected and stored at  $-30^{\circ}\text{C}$  until analysis. Organs were homogenized with 4% (w/v) bovine serum albumin and stored at  $-30^{\circ}\text{C}$  until analysis. Relative tissue-to-plasma ratios after oral administration were calculated by determining the larotrectinib tissue concentration relative to larotrectinib plasma concentration at the last time point.

#### 2.6. LC-MS/MS analysis

Larotrectinib concentrations in plasma samples and organ homogenates were determined using a validated liquid chromatography-tandem mass spectrometry assay [26].

#### 2.7. Data and statistical analysis

Pharmacokinetic parameters were calculated by non-compartmental methods using the PK Solver software [31]. The area under the plasma concentration–time curve (AUC) was calculated using the trapezoidal rule, without extrapolating to infinity. The peak plasma concentration ( $C_{\text{max}}$ ) and the time of maximum plasma concentration ( $T_{\text{max}}$ ) were estimated from the original (individual mouse) data. One-way analysis of variance (ANOVA) was used when multiple groups were compared and the Tukey post hoc correction was used to accommodate multiple

testing. The two-sided unpaired Student's *t*-test was used when treatments or differences between two specific groups were compared using the software GraphPad Prism 9 (GraphPad Software Inc., La Jolla, CA, USA). All the data were log-transformed before statistical tests were applied. Differences were considered statistically significant when  $P < 0.05$ . All data are presented as geometric mean  $\pm$  SD.

### 3. Results

#### 3.1. Effect of the dual ABCB1 and ABCG2 inhibitor elacridar on larotrectinib pharmacokinetics

It has been demonstrated in a previous study that mAbcb1a/1b and mAbcg2 together can markedly limit larotrectinib oral availability and brain accumulation [7]. In view of the potential benefit of further enhancing larotrectinib overall exposure and brain accumulation and drug disposition in other organs, it is useful to assess to what extent the dual ABCB1 and ABCG2 inhibitor elacridar could modulate the pharmacokinetics, especially plasma exposure and brain accumulation, of oral larotrectinib. Considering that the peak concentration of elacridar occurs approximately 4 h after oral administration [32], and that a dose of 100 mg/kg was virtually certain to provide complete inhibition of the BBB apical ABC transporters [33,34], elacridar (100 mg/kg) was administered orally 3 h prior to oral larotrectinib (10 mg/kg) to male wild-type and *Abcb1a/1b;Abcg2*<sup>-/-</sup> mice. Plasma and organ larotrectinib levels were assessed 1 h later. In vehicle-treated mice, the larotrectinib plasma AUC<sub>0–1h</sub> was significantly higher (2.3-fold) in *Abcb1a/1b;Abcg2*<sup>-/-</sup> compared to wild-type mice. Pre-treatment with elacridar increased the larotrectinib plasma exposure in wild-type mice to a similar level as seen in vehicle-treated *Abcb1a/1b;Abcg2*<sup>-/-</sup> mice, whereas it did not affect the plasma levels in *Abcb1a/1b;Abcg2*<sup>-/-</sup> mice (Fig. 1A,B). These results indicate that larotrectinib plasma exposure and oral availability in wild-type mice are markedly increased by elacridar, to the same levels as observed for the genetic knockout of *Abcb1a/1b* and *Abcg2*. This suggests effectively complete inhibition of these ABC transporters.

In the absence of elacridar, brain concentrations and brain-to-plasma ratios of larotrectinib were 15.9-fold and 6.3-fold higher in *Abcb1a/1b;Abcg2*<sup>-/-</sup> mice than in wild-type mice. Elacridar substantially increased the brain concentrations and brain-to-plasma ratios of larotrectinib in wild-type mice by 13.8-fold and 5.0-fold, respectively (Fig. 1C,D and Table 1), resulting in levels similar to those observed in *Abcb1a/1b;Abcg2*<sup>-/-</sup> mice with or without elacridar pretreatment. Elacridar did not significantly affect these parameters in *Abcb1a/1b;Abcg2*<sup>-/-</sup> mice, further supporting the specificity of elacridar in inhibiting *Abcb1* and *Abcg2* in the BBB. In view of the functional presence of ABCB1 and ABCG2 in the blood–testis barrier, testis distribution of larotrectinib was also analyzed. As shown in Supplemental Fig. 2B and Table 1, no significant differences in testis-to-plasma ratios were found among these groups, likely due in part to the high experimental variation in wild-type mice.

In liver, significantly lower liver-to-plasma ratios were observed in vehicle-treated *Abcb1a/1b;Abcg2*<sup>-/-</sup> mice compared to vehicle-treated wild-type mice. These results confirm a trend that was observed in the previous larotrectinib study. A reduced liver-to-plasma ratio in *Abcb1a/1b;Abcg2*<sup>-/-</sup> liver may indicate reduced accumulation of larotrectinib in intrahepatic bile due to the absence of the canalicular ABC transporters. Elacridar treatment yielded a similarly decreased liver-to-plasma ratio in wild-type mice as seen in vehicle- or elacridar-treated *Abcb1a/1b;Abcg2*<sup>-/-</sup> mice (Supplemental Fig. 2F and Table 1), consistent with specific inhibition of the hepatic ABC transporters. Somewhat similar results might perhaps occur in kidney, with the ABC transporters concentrating larotrectinib in the intrarenal pre-urine, but experimental variation did not allow a statistically significant conclusion here (Supplemental Fig. 2D).

In a previous study, about 3-fold reduced larotrectinib tissue-to-plasma ratios in the small intestinal tissue of *Abcb1a/1b;Abcg2*<sup>-/-</sup> mice

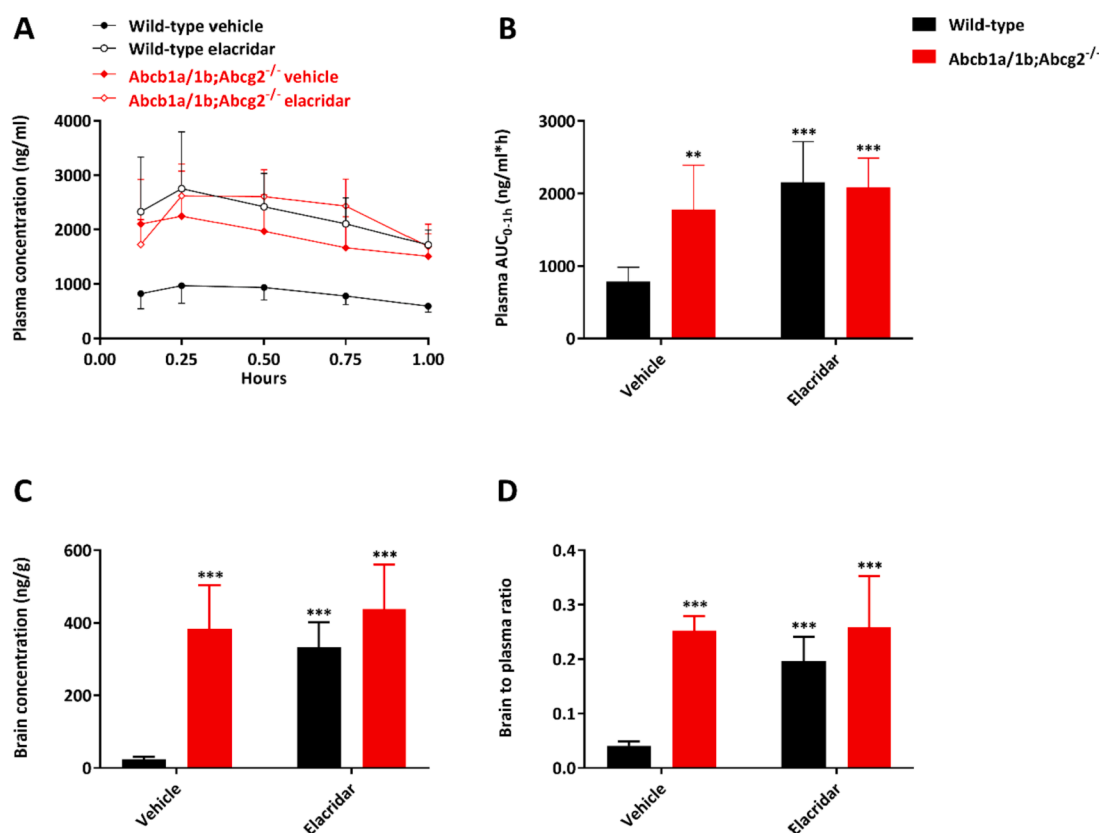


**Fig. 1.** Plasma concentration–time curves (A), plasma AUC<sub>0-1h</sub> (B), brain concentration (C) and brain-to-plasma ratio (D) of larotrectinib in male wild-type and *Abcb1a/1b;Abcg2<sup>-/-</sup>* mice over 1 h after oral administration of 10 mg/kg larotrectinib with or without co-administration of elacridar. Data are given as mean ± S.D. (n = 6). \*,  $P < 0.05$ ; \*\*,  $P < 0.01$ ; \*\*\*,  $P < 0.001$  compared to vehicle-treated wild-type mice.

were observed [7]. This usually reflects a strongly reduced drug concentration in the small intestinal content (SIC). Therefore, in this experiment, SI was collected together with the SIC. The results revealed a profoundly decreased concentration (13.9-fold), tissue-to-plasma ratio (35.2-fold), percentage of dose (6.0-fold) and percentage of dose-to-plasma ratio (16.9-fold) of larotrectinib in SI + SIC in vehicle-treated *Abcb1a/1b;Abcg2<sup>-/-</sup>* compared to wild-type mice. Pre-treatment with elacridar of wild-type mice led to very similar results, with concentration, tissue-to-plasma ratio, percentage of dose and percentage of dose-to-plasma ratio of larotrectinib decreased by 7.4-fold, 21.1-fold, 14.1-fold and 35.7-fold, respectively, compared to vehicle-treated wild-type mice (Supplemental Fig. 2G–J and Table 1). These results point to a more rapid and extensive absorption of intestinal larotrectinib upon inhibition of both *Abcb1a/1b* and *Abcg2*, or to reduced hepatobiliary excretion of the absorbed larotrectinib, or to a combination of both processes. Despite the overall increased plasma and tissue exposure, there was no sign of spontaneous toxicity of larotrectinib in any of the mouse strains tested with oral larotrectinib at 10 mg/kg, either in the absence or presence of elacridar.

Collectively, these data indicate that oral elacridar treatment can extensively and specifically inhibit the activity of mouse *Abcb1* and *Abcg2* in the BBB, leading to markedly increased larotrectinib distribution to the brain at an early time point, when the larotrectinib exposure was relatively high. Moreover, elacridar could markedly enhance the general oral exposure of larotrectinib, presumably mainly due to increased net drug absorption from the gut or reduced hepatobiliary excretion, or both.

### 3.2. Impact of human *SLCO1B1* and *1B3* on larotrectinib pharmacokinetics

To investigate the possible impact of human OATP1B1 and OATP1B3 on oral bioavailability and tissue disposition of larotrectinib, a 1 h pharmacokinetic study in male wild-type, *Slco1a/1b<sup>-/-</sup>*, *SLCO1B1* and *SLCO1B3* mice was performed, using oral administration of 10 mg/kg larotrectinib. *SLCO1B1* and *SLCO1B3* mice are *Slco1a/1b<sup>-/-</sup>* mice that transgenically overexpress human OATP1B1 or *-1B3* in the liver, respectively. As shown in Fig. 2A–B and Supplemental Table 1, absorption was very rapid and the  $T_{max}$  occurred between 0.25 and 0.75 h in all four strains. The plasma exposure of larotrectinib over 1 h (AUC<sub>0-1h</sub>) was significantly higher (2.5-fold) in *Slco1a/1b<sup>-/-</sup>* mice than in wild-type mice, in line with the preceding study [7]. However, *SLCO1B1* and *SLCO1B3* did not decrease the plasma exposure of larotrectinib, with the plasma AUC<sub>0-1h</sub> still 2.7-fold and 2.5-fold increased, respectively, compared to wild-type mice.

Brain, liver, kidney, lung, small intestine and testis concentrations of larotrectinib 1 h after oral administration were also analyzed. Due to the higher plasma exposure of larotrectinib in *Slco1a/1b<sup>-/-</sup>*, *SLCO1B1* and *SLCO1B3* mice, brain, kidney, lung and testis had higher drug concentrations in all of these three mouse strains. However, the relative tissue-to-plasma ratios revealed no meaningful differences among all the mouse strains for brain, testis, and kidney, although there was a consistent modest reduction in relative lung distribution in all the *Oatp1a/1b*-deficient mouse strains (Supplemental Fig. 3). The latter finding is in line with what was observed in the preceding larotrectinib study [7], and suggests that possibly *Oatp1a/1b* proteins play a limited role in distribution of larotrectinib to lung tissue. Whereas the liver concentrations showed no differences between all strains, this translated into significantly lower liver-to-plasma ratios in *Slco1a/1b<sup>-/-</sup>*, *SLCO1B1*

**Table 1**

Plasma and tissue pharmacokinetic parameters of larotrectinib in male wild-type and *Abcb1a/1b;Abcg2*<sup>-/-</sup> mice over 1 h after oral administration of 10 mg/kg larotrectinib with or without inhibitor elacridar.

Parameter	Genotype/Groups			
	Vehicle		Elacridar	
	Wild-type	<i>Abcb1a/1b;Abcg2</i> <sup>-/-</sup>	Wild-type	<i>Abcb1a/1b;Abcg2</i> <sup>-/-</sup>
AUC <sub>0-1h</sub> , ng/ml·h	787 ± 196	1781 ± 611**	2153 ± 563***	2086 ± 403***
Fold change	1.0	2.3	2.7	2.7
C <sub>max</sub> , ng/ml	1008 ± 304	2262 ± 832**	2871 ± 963***	2749 ± 518***
T <sub>max</sub> , h	0.38 ± 0.14	0.27 ± 0.12	0.36 ± 0.23	0.46 ± 0.19
C <sub>brain</sub> , ng/g	24.1 ± 7.2	383.4 ± 121***	333.0 ± 68.3***	437.6 ± 123.3***
Fold increase	1.0	15.9	13.8	18.2
C <sub>brain</sub>				
Brain-to-plasma ratio	0.040 ± 0.009	0.25 ± 0.03***	0.20 ± 0.04***	0.26 ± 0.09***
Fold increase	1.0	6.3	5.0	6.5
C <sub>liver</sub> , ng/g	4564 ± 410	6458 ± 1516*	8746 ± 2147***	9003 ± 1487***
Fold increase	1.0	1.4	1.9	2.0
C <sub>liver</sub>				
Liver-to-plasma ratio	7.9 ± 1.2	4.3 ± 0.5***	5.1 ± 0.6***	5.3 ± 1.1***
Fold change	1.0	0.54	0.65	0.67
C <sub>SI + SIC</sub> , ng/g	42565 ± 7747	3060 ± 427***	5770 ± 1169***	5737 ± 2926***
Fold increase	1.0	0.072	0.14	0.13
C <sub>SI + SIC</sub>				
SI + SIC-to-plasma ratio	73.9 ± 17.8	2.1 ± 0.6***	3.5 ± 1.1***	3.2 ± 1.2***
Fold change	1.0	0.028	0.047	0.043
C <sub>testis</sub> , ng/g	170.6 ± 99.6	578.4 ± 177.1***	502.5 ± 125.8***	843.9 ± 212.2***
Fold increase	1.0	3.4	2.9	4.9
C <sub>testis</sub>				
Testis-to-plasma ratio	0.29 ± 0.19	0.38 ± 0.02	0.29 ± 0.07	0.50 ± 0.19*
Fold change	1.0	1.3	1.0	1.7
ratio				

Data are given as mean ± S.D. (n = 6). AUC<sub>0-1h</sub>, area under the plasma concentration–time curve; C<sub>max</sub>, maximum concentration in plasma; T<sub>max</sub>, time point (h) of maximum plasma concentration; C<sub>brain</sub>, brain concentration; C<sub>liver</sub>, liver concentration; SI, small intestine (tissue); SIC, small intestine contents; C<sub>SI + SIC</sub>, small intestine tissue together with small intestine contents concentration; C<sub>testis</sub>, testis concentration; \*, P < 0.05; \*\*, P < 0.01; \*\*\*, P < 0.001 compared to vehicle-treated wild-type mice. Statistical analysis was applied after log-transformation of linear data.

and Slco1B3 compared to wild-type mice (2.7-fold, 2.7-fold and 2.4-fold, respectively (Fig. 2C,D and Supplemental Table 1). This is in line with a clear role for mOatp1a/1b proteins in the liver uptake of larotrectinib, but not for human OATP1B1 or –1B3. With respect to small intestinal tissue concentration, even though this was 1.7-fold higher in *Slco1a/1b*<sup>-/-</sup> mice than in wild-type mice, and slightly higher in SLCO1B1 (1.2-fold) and SLCO1B3 (1.3-fold) mice, no significant difference showed up among all the mouse strains. However, as also seen for the liver, small intestine-to-plasma ratios were significantly reduced in *Slco1a/1b*<sup>-/-</sup>, SLCO1B1 and SLCO1B3 mice compared to wild-type mice (2-fold, 2.8-fold and 2.4-fold, respectively. Fig. 2E,F and Supplemental Table 1). Such intestinal tissue data shortly after oral administration of drugs often primarily reflect the intestinal content levels (which were not measured in this experiment). These data therefore suggest that the uptake function of mouse Oatp1a/1b proteins for larotrectinib in the

liver indirectly also affects the intestinal (content) exposure through hepatobiliary excretion, but that human OATP1B1 and OATP1B3 do not. All in all, the collected data thus further support that larotrectinib is not a transport substrate of hepatic human OATP1B1 and OATP1B3 *in vivo*.

### 3.3. Larotrectinib pharmacokinetic behavior after co-administration of the OATP inhibitor rifampin

The potential influence of rifampin, an Slco1a/1b inhibitor, on larotrectinib pharmacokinetics *in vivo* was investigated next. Aiming for relatively high plasma and tissue levels for both larotrectinib and rifampin when assessing larotrectinib tissue distribution, a 1 h pharmacokinetic experiment in wild-type, *Slco1a/1b*<sup>-/-</sup>, SLCO1B1 and SLCO1B3 mice was performed, with rifampin (100 mg/kg) or vehicle orally administered 15 min prior to oral larotrectinib at 10 mg/kg. Both vehicle-treated *Slco1a/1b*<sup>-/-</sup> mice and rifampin-treated wild-type mice showed a higher larotrectinib plasma AUC<sub>0-1h</sub> than vehicle-treated wild-type mice (each 1.9-fold higher). This suggests that rifampin could inhibit mouse Oatp1a/1b and thus increase larotrectinib plasma exposure (Fig. 3A,B). However, it is worth noticing that after pre-treatment with rifampin, larotrectinib plasma exposure also increased in *Slco1a/1b*<sup>-/-</sup> mice compared with vehicle-treated *Slco1a/1b*<sup>-/-</sup> mice. Meanwhile, SLCO1B1 and SLCO1B3 mice showed a significantly higher plasma AUC<sub>0-1h</sub> compared to wild-type mice and a similar plasma AUC<sub>0-1h</sub> of larotrectinib no matter whether in the vehicle- or rifampin-treated group (Fig. 3).

To try and come to a better mechanistic understanding of these observations, organs were collected after 1 h and larotrectinib concentrations were measured. Brain, testis and kidney mostly reflected the plasma larotrectinib exposure and no meaningful changes showed up in tissue-to-plasma ratios in either vehicle- or rifampin-treated groups (Supplemental Fig. 4). While there were no differences in absolute larotrectinib concentrations among all four mouse strains in either vehicle- or rifampin-treated groups, the liver-to-plasma ratios were significantly decreased in *Slco1a/1b*<sup>-/-</sup>, SLCO1B1 and SLCO1B3 mice in the vehicle-treated group. This suggests a relatively reduced liver uptake of larotrectinib in *Slco1a/1b*<sup>-/-</sup> mice and no substantial uptake functions of human OATP1B1 and OATP1B3. Importantly, the rifampin-treated group wild-type mice had a similar liver-to-plasma ratio as the vehicle-treated *Slco1a/1b*<sup>-/-</sup> mice (3.7 ± 0.5 vs 3.6 ± 0.6). This suggests that rifampin could effectively inhibit the mouse hepatic *Slco1a/1b* proteins and thus restrict liver uptake of larotrectinib (Supplemental Figure 5B and Table 2).

In this experiment the small intestine (SI) and its content (SIC) combined (SI + SIC) were also measured. In vehicle-treated groups, SI + SIC-to-plasma ratios in *Slco1a/1b*<sup>-/-</sup> (37.2 ± 14.2), SLCO1B1 (25.1 ± 8.0) and SLCO1B3 (25.7 ± 8.5) mice were not significantly changed compared to wild-type mice (43.7 ± 27.2) (Supplemental Figure 5D). Interestingly, pre-treatment with rifampin could markedly decrease these ratios in all the groups to a similar level. Similarly, the amount of larotrectinib recovered from SI + SIC as percentage of the dose-to-plasma ratios was also clearly reduced in all the rifampin-treated groups compared to corresponding vehicle-treated groups (Supplemental Figure 5F). These data suggest that rifampin had an additional impact on larotrectinib intestinal disposition that was not directly related to inhibition of Oatp1a/1b-mediated liver uptake. The most likely explanation is that the high intestinal concentration of (oral) rifampin also inhibited the intestinal Abcb1 and perhaps Abcg2 proteins, thus increasing the net rate of uptake of larotrectinib from the intestinal lumen. Furthermore, likely the extent of inhibition of ABC transporters in other organs that were only exposed to rifampin through the blood did not affect larotrectinib excretion much, resulting in only a limited increase in overall plasma exposure in *Slco1a/1b*<sup>-/-</sup>, Slco1B1 and Slco1B3 mice. Nonetheless, considering that the elimination phase started within 1 h, it may be that additional Abcb1 inhibition by rifampin was responsible for the relative increase in plasma AUC in the

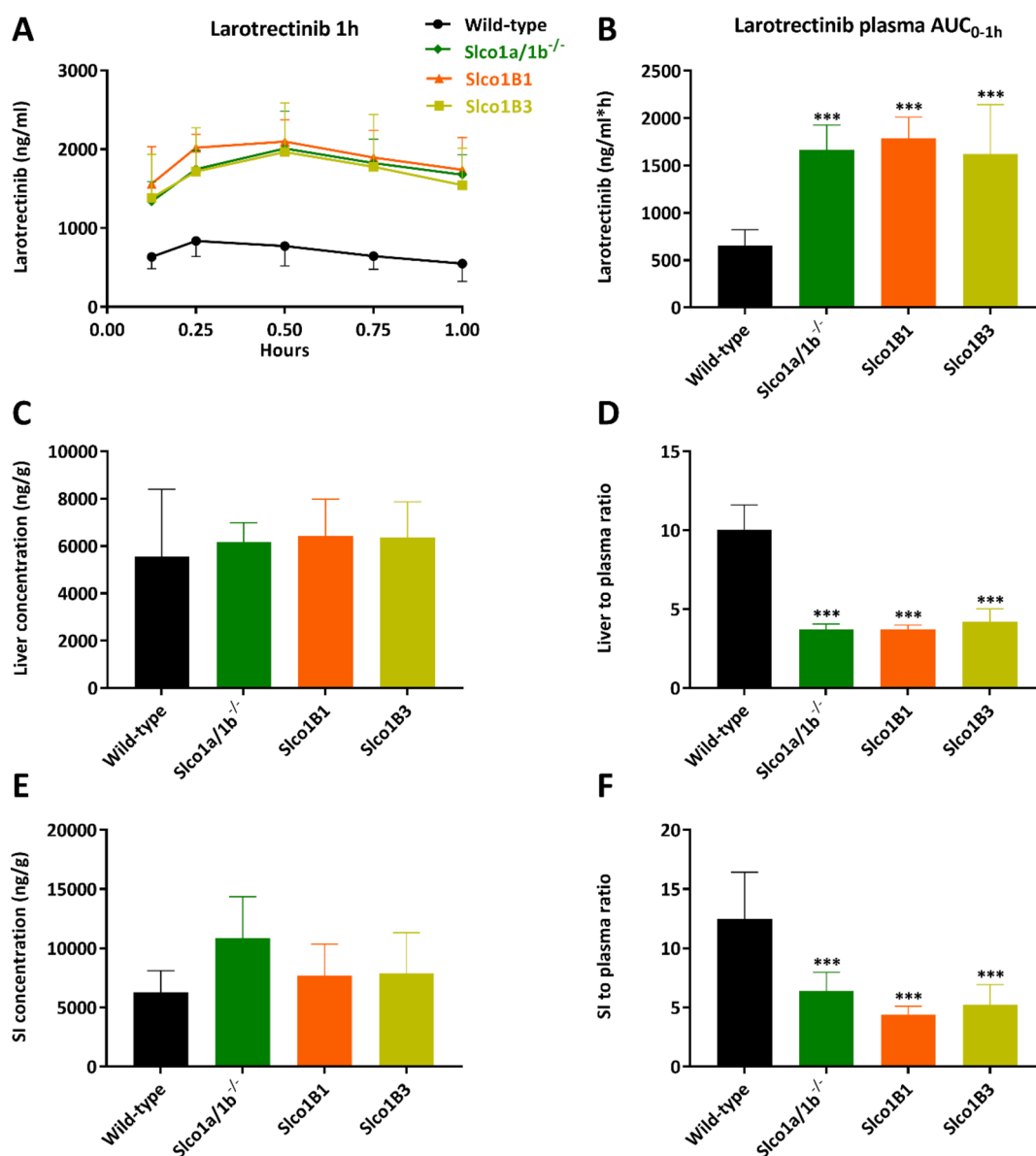


**Fig. 2.** Plasma concentration–time curves (A), plasma AUC<sub>0-1h</sub> (B), liver concentration (C), liver-to-plasma ratio (D), small intestine concentration (E) and small intestine-to-plasma ratio (F) of larotrectinib in male wild-type, *Slco1a/1b*<sup>-/-</sup>, *Slco1B1* and *Slco1B3* mice over 1 h after oral administration of 10 mg/kg larotrectinib. SI: Small intestine. Data are given as mean  $\pm$  S.D. (n = 6–7). \*,  $P < 0.05$ ; \*\*,  $P < 0.01$ ; \*\*\*,  $P < 0.001$  compared to wild-type mice.

*Slco1a/1b*<sup>-/-</sup> mice (Fig. 3B). Of note, no acute toxicity complications of larotrectinib were observed in any of the mouse strains tested with oral larotrectinib at 10 mg/kg, either in the absence or in the presence of rifampin.

### 3.4. Larotrectinib exposure and tissue distribution upon co-administration with the CYP3A inhibitor ritonavir

In order to examine whether the oral availability of larotrectinib could be increased by inhibition of CYP3A, the irreversible CYP3A inhibitor ritonavir (50 mg/kg) or vehicle was administered orally 15 min prior to oral larotrectinib (15 mg/kg) to male wild-type, *Cyp3a*<sup>-/-</sup>, and *Cyp3aXAV* mice, which express transgenic human CYP3A4 in liver and intestine of *Cyp3a*<sup>-/-</sup> mice. In vehicle-treated mice, although the plasma AUC<sub>0-1h</sub> was not statistically significantly different among the three mouse strains, it was modestly increased (1.4-fold) in *Cyp3a*<sup>-/-</sup> mice and then relatively decreased (by 1.7-fold) in *Cyp3aXAV* mice (Fig. 4 and Table 3), similar to the previously observed significant plasma AUC<sub>0-4h</sub> differences among these strains measured over 4 h [7]. While the plasma

AUC differences were not significant, the larotrectinib tissue concentrations at 1 h among these three strains clearly supported an increase in exposure in *Cyp3a*<sup>-/-</sup> mice relative to wild-type mice, and a subsequent strong decrease in *Cyp3aXAV* mice (Supplemental Figures 6 and 7). This applied to all tested tissues, i.e. brain, testis, kidney, liver, and SI + SIC.

In the absence of ritonavir, brain-, testis- and kidney-to-plasma ratios of larotrectinib were similar among wild-type, *Cyp3a*<sup>-/-</sup> and *Cyp3aXAV* mice, suggesting that the CYP3A genotype did not influence the distribution between tissue and blood in these organs (Supplemental Figure 6). However, there were clear increases in liver- and SI + SIC-to-plasma ratios in *Cyp3a*<sup>-/-</sup> mice (1.3-fold,  $P < 0.05$  and 2.0-fold,  $P < 0.01$ ) compared to wild-type mice and then downward shifts in *Cyp3aXAV* mice (0.7-fold,  $P < 0.01$  and 0.3-fold,  $P < 0.001$ ) relative to *Cyp3a*<sup>-/-</sup> mice (Supplemental Figure 7 and Table 3). These effects might be related to the direct metabolism of larotrectinib by Cyp3a and CYP3A4 enzymes in liver and intestinal tissue. Overall, these data support our earlier finding that transgenic human CYP3A4 has a substantial impact on larotrectinib pharmacokinetics, as does endogenous mouse Cyp3a.

Unexpectedly, pre-treatment with ritonavir resulted in plasma

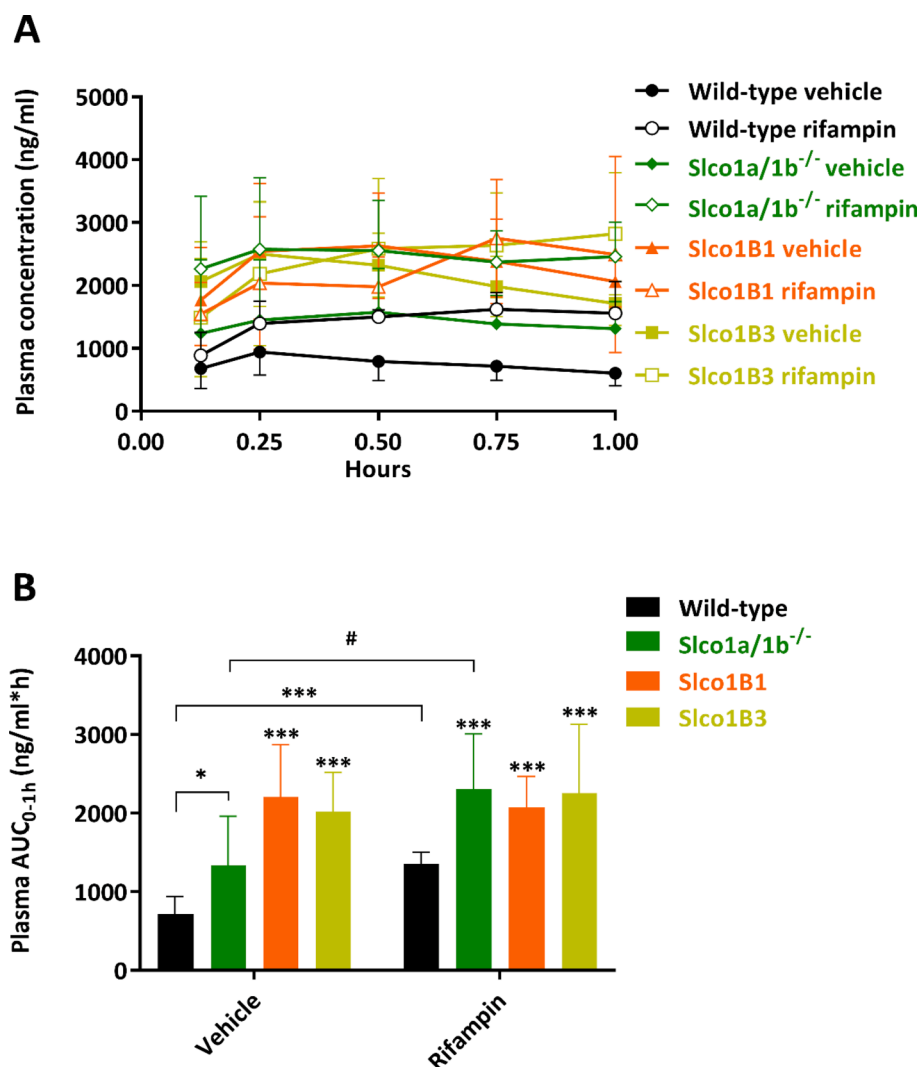


**Fig. 3.** Plasma concentration–time curves (A) and plasma AUC<sub>0-1h</sub> (B) of larotrectinib in male wild-type, *Slco1a/1b*<sup>-/-</sup>, *Slco1B1* and *Slco1B3* mice over 1 h after oral administration of 10 mg/kg larotrectinib with or without co-administration of rifampin. Data are given as mean ± S.D. (n = 6–7). \*,  $P < 0.05$ ; \*\*,  $P < 0.01$ ; \*\*\*,  $P < 0.001$  compared to vehicle-treated wild-type mice; #,  $P < 0.05$  compared between vehicle-treated and rifampin-treated *Slco1a/1b*<sup>-/-</sup> mice; No significant differences were observed between vehicle-treated *Slco1B1* and rifampin-treated *Slco1B1* mice or between vehicle-treated *Slco1B3* and rifampin-treated *Slco1B3* mice.

larotrectinib exposure increases not only in wild-type mice (1.5-fold compared to vehicle-treated wild-type mice) and *Cyp3aXAV* mice (2.2-fold compared to vehicle-treated *Cyp3aXAV* mice), but also in *Cyp3a*<sup>-/-</sup> mice (1.7-fold compared to vehicle-treated *Cyp3a*<sup>-/-</sup> mice) (Fig. 4 and Table 3). These shifts suggest that ritonavir must have additional effects beyond the possible inhibition of mouse *Cyp3a* (and human CYP3A4). Brain, testis and kidney absolute drug concentrations were also increased, but ritonavir had no substantial influence on the relative brain-, testis- and kidney-to-plasma ratios in these three mouse strains (Supplemental Figure 6). The increases in concentrations in these tissues therefore mainly reflected the higher plasma levels of larotrectinib due to ritonavir treatment. In contrast, for both liver and small intestine with intestinal contents, a marked decrease in tissue-to-plasma ratios was observed to a similar level in all of the three mouse strains upon pretreatment with ritonavir (Supplemental Figure 7). These results suggest that, in addition to *Cyp3a*/*CYP3A4*, also some other larotrectinib-handling systems were noticeably affected by ritonavir in liver and intestine. Given that *Abcb1a/1b*/*Abcg2* deficiency likewise resulted in decreased liver-to-plasma ratios and SI + SIC-to-plasma ratios (Supplemental Fig. 2), and as ritonavir is known to inhibit *ABCB1* P-glycoprotein, a likely explanation is that ritonavir also inhibited *Abcb1a/1b* activity in intestine and liver.

#### 4. Discussion and conclusions

In a preceding more detailed pharmacokinetic study [7], larotrectinib was shown to be efficiently transported by *ABCB1* and *ABCG2*, and affected by *Oatp1a/1b* proteins as well as *CYP3A4*. One conclusion from that study was that the main differences in plasma AUC between the strains developed during the first hour after larotrectinib administration. For that reason, as three different perpetrator drugs were used in the current drug-drug interaction analysis in several different mouse strains, this work focused on one-hour studies. This also allowed assessment of the role of changes in tissue distribution of larotrectinib at a time point when its plasma concentration was still relatively high.

In the current study it was found that the dual *ABCB1* and *ABCG2* inhibitor elacridar could extensively enhance the plasma exposure and especially the brain penetration of larotrectinib in wild-type mice, but not in *Abcb1a/1b*/*Abcg2*<sup>-/-</sup> mice. This suggests that these pharmacokinetic effects of elacridar were specifically mediated by virtually complete inhibition of these ABC transporters. In contrast, in liver elacridar decreased the liver-to-plasma ratios in wild-type mice, yielding similarly reduced ratios as seen in vehicle-treated *Abcb1a/1b*/*Abcg2*<sup>-/-</sup> mice. Previously similar hepatic distribution effects were noticed for some other small-molecular inhibitors (TKIs) that are ABC transporter substrates. The likely cause is high accumulation of larotrectinib in intrahepatic bile due to the concentrative effect of the ABC transporters, resulting in higher overall liver concentration of larotrectinib in wild-type liver than

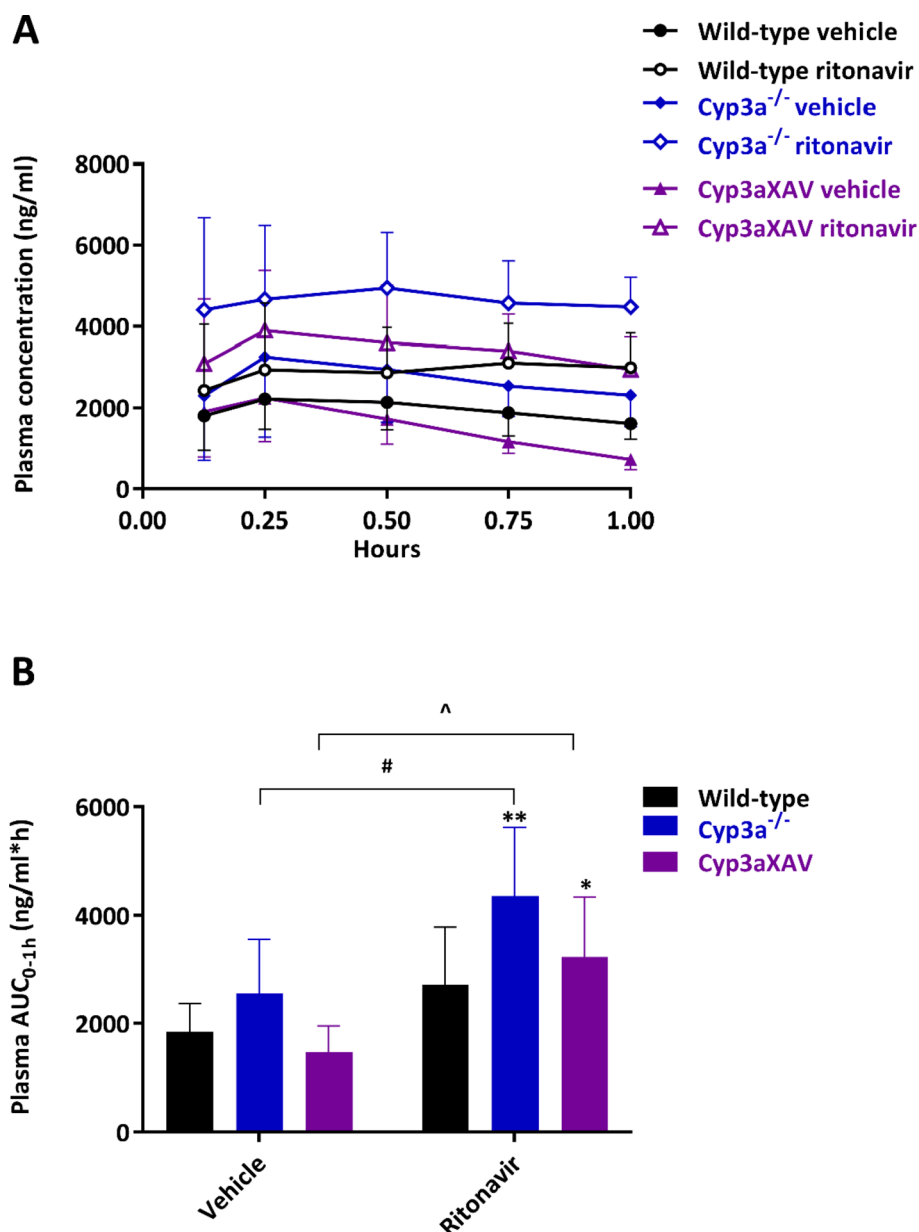


**Fig. 4.** Plasma concentration–time curves (A) and plasma AUC<sub>0-1h</sub> (B) of larotrectinib in male wild-type, Cyp3a<sup>-/-</sup> and Cyp3aXAV mice over 1 h after oral administration of 15 mg/kg larotrectinib with or without co-administration of ritonavir. Data are given as mean ± S.D. (n = 6). \*,  $P < 0.05$ ; \*\*,  $P < 0.01$  compared to vehicle-treated wild-type mice; #,  $P < 0.05$  compared between vehicle-treated and ritonavir-treated Cyp3a<sup>-/-</sup> mice; ^,  $P < 0.05$  compared between vehicle-treated and ritonavir-treated Cyp3aXAV mice.

in ABC-transporter-deficient liver [35]. These results thus suggest extensive inhibition of bile canalicular Abcb1a/1b and Abcg2 by elacridar treatment. Pre-treatment with elacridar further lead to a marked decrease in drug concentration and percentage of dose in SI + SIC and related parameters, also after correction for the plasma levels in wild-type mice compared to vehicle-treated wild-type mice. This indicates that elacridar could further extensively inhibit intestinal Abcb1a/1b and Abcg2 activity. No noticeable changes in tissue distribution due to the ABC transporter deficiencies were found in other tissues. As several of the cancers indicated for larotrectinib treatment reside in the brain or readily form brain metastases, it may be considered to coadminister elacridar in order to improve the brain penetration and thus possibly therapeutic efficacy of larotrectinib.

It was further found previously that larotrectinib was a likely substrate of human OATP1A2 *in vitro*, but not of human OATP1B1 or –1B3 [7]. To further investigate the possible impact of OATPs on larotrectinib behavior *in vivo*, a distribution study in human SLCO1B1 or SLCO1B3 transgenic mice was performed with wild-type and *Slco1a/1b*<sup>-/-</sup> mice as controls. The results confirmed that larotrectinib is taken up into the

liver by the mouse Oatp1a/1b proteins, and that this secondarily results in higher intestinal levels of larotrectinib. However, there were no indications for an analogous function of hepatic transgenic human OATP1B1 or OATP1B3. This indicates that larotrectinib is not a substrate of human OATP1B1 or 1B3 *in vivo*, consistent with the FDA registration documentation [5]. A modest reduction in larotrectinib uptake was further observed in lungs of *Slco1a/1b*<sup>-/-</sup> mice, as also seen in a previous study [7]. This suggests a limited impact of mOatp1a/1b on larotrectinib lung uptake.

Rifampin, a well-studied OATP inhibitor, can dramatically influence the pharmacokinetics of OATP substrate drugs. It was demonstrated previously that in mice rifampin (20 mg/kg i.v. injection) was an effective and specific Oatp1a/1b inhibitor in controlling methotrexate pharmacokinetics [28]. In the current study, keeping in line with the clinical usage (oral administration in most cases), rifampin was administered orally at a high dose of 100 mg/kg shortly (15 min) before larotrectinib, aiming for high intestinal and liver concentrations of rifampin during, and shortly after, larotrectinib administration. The results indicate that rifampin decreased the relative liver uptake in wild-

**Table 2**

Plasma and tissue pharmacokinetic parameters of larotrectinib in male wild-type, *Slco1a/1b*<sup>-/-</sup>, *Slco1B1* and *Slco1B3* mice over 1 h after oral administration of 10 mg/kg larotrectinib with or without inhibitor rifampin.

Parameter	Genotype/Groups							
	Vehicle				Rifampin			
	Wild-type	<i>Slco1a/1b</i> <sup>-/-</sup>	<i>Slco1B1</i>	<i>Slco1B3</i>	Wild-type	<i>Slco1a/1b</i> <sup>-/-</sup>	<i>Slco1B1</i>	<i>Slco1B3</i>
AUC <sub>0-1h</sub> , ng/ml.h	715 ± 227	1333 ± 627*	2210 ± 662***	2019 ± 499***	1351 ± 155***	2306 ± 703***	2071 ± 399***	2255 ± 875***
Fold change AUC <sub>0-1h</sub>	1.0	1.9	3.1	2.8	1.9	3.2	2.9	3.2
C <sub>max</sub> , ng/ml	977 ± 321	1779 ± 881*	2800 ± 962***	2557 ± 781***	1857 ± 329**	2955 ± 702***#	3197 ± 1457***	3026 ± 1052***
T <sub>max</sub> , h	0.46 ± 0.3	0.46 ± 0.4	0.54 ± 0.3	0.33 ± 0.1	0.71 ± 0.3	0.54 ± 0.4	0.67 ± 0.3	0.71 ± 0.4
C <sub>brain</sub> , ng/g	21.2 ± 2.8	44.9 ± 16.7	68.0 ± 27.2***	70.2 ± 19.6***	84.9 ± 30.4***	139.6 ± 45.7***###	102.9 ± 52.9***	129.7 ± 69.9***
Fold increase C <sub>brain</sub>	1.0	2.1	3.2	3.3	4.0	6.6	4.9	6.1
Brain-to-plasma ratio	0.039 ± 0.02	0.037 ± 0.02	0.033 ± 0.01	0.042 ± 0.01	0.057 ± 0.02	0.057 ± 0.01#	0.052 ± 0.03	0.045 ± 0.02
Fold change ratio	1.0	0.95	0.85	1.1	1.5	1.5	1.3	1.2
C <sub>liver</sub> , ng/g	4812 ± 1392	4628 ± 1584	6265 ± 1393	6676 ± 2124	5555 ± 1192	8316 ± 946***##	6383 ± 1084	6875 ± 810**
Fold increase C <sub>liver</sub>	1.0	1.0	1.3	1.4	1.2	1.7	1.3	1.1
Liver-to-plasma ratio	8.1 ± 0.8	3.6 ± 0.6***	3.0 ± 0.2***	3.9 ± 1.1***	3.7 ± 0.5***	3.5 ± 0.5***	3.2 ± 1.2***^	2.2 ± 1.4***
Fold change ratio	1.0	0.44	0.37	0.48	0.46	0.43	0.40	0.27
C <sub>SI + SIC</sub> , µg/g	23.7 ± 10.5	44.3 ± 5.4*	50.4 ± 11.1**	42.7 ± 12.8*	13.0 ± 3.7	20.3 ± 4.5###	18.6 ± 2.7***	27.2 ± 7.6^
Fold change C <sub>SI + SIC</sub>	1.0	1.9	2.1	1.8	0.5	0.9	0.8	1.1
SI + SIC-to-plasma ratio	43.7 ± 27.2	37.2 ± 14.2	25.1 ± 8.0	25.7 ± 8.5	8.4 ± 1.2***	8.5 ± 1.7***	9.3 ± 3.5***	9.9 ± 1.6***
Fold change ratio	1.0	0.85	0.57	0.59	0.19	0.19	0.21	0.23
C <sub>testis</sub> , ng/g	175.2 ± 103.7	328.4 ± 148.7	534.3 ± 128.8**	411.5 ± 71.6**	358.1 ± 141.3*	326.3 ± 72.9*	337.8 ± 74.5**	369.1 ± 112.0*
Fold increase C <sub>testis</sub>	1.0	1.9	3.0	2.3	2.0	1.9	1.9	2.1
Testis-to-plasma ratio	0.35 ± 0.32	0.26 ± 0.12	0.26 ± 0.04	0.25 ± 0.08	0.23 ± 0.04	0.13 ± 0.03#	0.17 ± 0.07	0.14 ± 0.04^
Fold change ratio	1.0	0.74	0.74	0.71	0.66	0.37	0.49	0.40

Data are given as mean ± S.D. (n = 6–7). AUC<sub>0-1h</sub>, area under the plasma concentration–time curve; C<sub>max</sub>, maximum concentration in plasma; T<sub>max</sub>, time point (h) of maximum plasma concentration; C<sub>brain</sub>, brain concentration; C<sub>liver</sub>, liver concentration; SI, small intestine (tissue); SIC, small intestine contents; C<sub>SI + SIC</sub>, small intestine tissue together with small intestine contents concentration; C<sub>testis</sub>, testis concentration; \*, P < 0.05; \*\*, P < 0.01; \*\*\*, P < 0.001 compared to vehicle-treated wild-type mice; #, P < 0.05; ##, P < 0.01; ###, P < 0.001 compared between vehicle-treated and rifampin-treated *Slco1a/1b*<sup>-/-</sup> mice; ^, P < 0.05; ^, P < 0.01; ^, P < 0.001 compared between vehicle-treated *Slco1B1* and rifampin-treated *Slco1B1* mice or between vehicle-treated *Slco1B3* and rifampin-treated *Slco1B3* mice. Statistical analysis was applied after log-transformation of linear data.

**Table 3**

Pharmacokinetic parameters, brain concentrations, and brain-to-plasma ratios of larotrectinib in male wild-type, *Cyp3a*<sup>-/-</sup> and *Cyp3aXAV* mice over 1 h after oral administration of 15 mg/kg larotrectinib with or without inhibitor ritonavir.

Parameter	Genotype/Groups					
	Vehicle			Ritonavir		
	Wild-type	<i>Cyp3a</i> <sup>-/-</sup>	<i>Cyp3aXAV</i>	Wild-type	<i>Cyp3a</i> <sup>-/-</sup>	<i>Cyp3aXAV</i>
AUC <sub>0-1h</sub> , ng/ml.h	1845 ± 530	2557 ± 1006	1470 ± 490	2719 ± 1067	4362 ± 1262***#	3232 ± 1113**
Fold change AUC <sub>0-1h</sub>	1.0	1.4	0.80	1.5	2.4	1.8
C <sub>max</sub> , ng/ml	2395 ± 763	3916 ± 1046*	2498 ± 856	3562 ± 1033	5314 ± 1377**	4040 ± 1306*
T <sub>max</sub> , h	0.50 ± 0.31	0.50 ± 0.39	0.40 ± 0.32	0.63 ± 0.34	0.52 ± 0.32	0.38 ± 0.21
C <sub>brain</sub> , ng/g	63.0 ± 35.7	84.1 ± 29.8	30.8 ± 9.9	143.8 ± 49.0*	284.1 ± 120.5***###	167.5 ± 44.3***^
Fold change C <sub>brain</sub>	1.0	1.3	0.49	2.3	4.5	2.7
Brain-to-plasma ratio	0.037 ± 0.01	0.039 ± 0.02	0.046 ± 0.02	0.049 ± 0.02	0.064 ± 0.03*	0.058 ± 0.01*
Fold change ratio	1.0	1.1	1.2	1.3	1.7	1.6
C <sub>liver</sub> , µg/g	15.0 ± 3.0	30.2 ± 14.6*	6.0 ± 1.5***	11.5 ± 2.9	19.3 ± 3.8	14.7 ± 3.5***
Fold change C <sub>liver</sub>	1.0	2.0	0.40	0.77	1.3	0.98
Liver-to-plasma ratio	9.4 ± 1.5	12.5 ± 2.5*	8.8 ± 2.8	3.9 ± 0.4***	4.3 ± 0.4***###	5.0 ± 0.4***^
Fold change ratio	1.0	1.3	0.94	0.41	0.46	0.53
C <sub>SI + SIC</sub> , µg/g	76.9 ± 40.1	222.5 ± 98.2**	20.9 ± 7.5**	24.2 ± 6.8**	58.5 ± 6.4###	45.4 ± 13.5**
Fold change C <sub>SI + SIC</sub>	1.0	2.9	0.27	0.31	0.76	0.59
SI + SIC-to-plasma ratio	47.3 ± 19.0	94.5 ± 21.0**	30.3 ± 8.7	8.4 ± 1.9***	13.2 ± 1.7***###	15.9 ± 5.4***^
Fold change ratio	1.0	2.0	0.64	0.18	0.28	0.34
C <sub>testis</sub> , ng/g	381.9 ± 240.8	699.8 ± 359.2	258.4 ± 87.5	772.1 ± 474.6	1518 ± 579.1***#	1195 ± 445.5***
Fold change C <sub>testis</sub>	1.0	1.8	0.68	2.0	4.0	3.1
Testis-to-plasma ratio	0.23 ± 0.13	0.40 ± 0.38	0.43 ± 0.28	0.25 ± 0.11	0.35 ± 0.16	0.40 ± 0.10*
Fold change ratio	1.0	1.7	1.9	1.1	1.5	1.7

Data are given as mean ± S.D. (n = 6). AUC<sub>0-1h</sub>, area under the plasma concentration–time curve; C<sub>max</sub>, maximum concentration in plasma; T<sub>max</sub>, time point (h) of maximum plasma concentration; C<sub>brain</sub>, brain concentration; C<sub>liver</sub>, liver concentration; SI, small intestine (tissue); SIC, small intestine contents; C<sub>SI + SIC</sub>, small intestine tissue together with small intestine contents concentration; C<sub>testis</sub>, testis concentration; \*, P < 0.05; \*\*, P < 0.01; \*\*\*, P < 0.001 compared to vehicle treated wild-type mice; #, P < 0.05; ##, P < 0.01; ###, P < 0.001 compared between vehicle-treated and ritonavir-treated *Cyp3a*<sup>-/-</sup> mice; ^, P < 0.05; ^, P < 0.01; ^, P < 0.001 compared between vehicle-treated and ritonavir-treated *Cyp3aXAV* mice. Statistical analysis was applied after log-transformation of linear data.

type mice by about 2.2-fold to similar levels as seen in *Slco1a/1b*<sup>-/-</sup> mice (Supplemental Figure 5B), resulting in a concomitant (~1.9-fold) increase in larotrectinib plasma levels (Fig. 3). As rifampin did not affect relative liver distribution of larotrectinib in *Slco1a/1b*<sup>-/-</sup> mice, this inhibitory effect appeared to be specific for the hepatic Oatp1a/1b proteins, with no other hepatic uptake or efflux transporters noticeably inhibited.

Based on the reduced relative liver uptake of larotrectinib and thus presumably reduced hepatobiliary excretion, it was expected that the SI + SIC values would also be reduced by rifampin treatment, as seen when comparing vehicle-treated wild-type and *Slco1a/1b*<sup>-/-</sup> mice. Surprisingly, however, the larotrectinib concentration and percentage of the dose in SI + SIC were significantly decreased in all the groups upon rifampin treatment, even in *Slco1a/1b*<sup>-/-</sup> mice, and these decreases were even more obvious after correction for plasma levels (Supplemental Figure 5D). These results indicate that, besides inhibiting hepatic Oatp1a/1b transporters, other larotrectinib-handling systems must have been influenced by rifampin. It is known that oral rifampin can inhibit enterocyte ABCB1 (P-gp), without affecting hepatic ABCB1 or renal transporters [21,36], thus inhibiting the efflux of digoxin, an excellent ABCB1 substrate, into the intestinal lumen. As larotrectinib is also an excellent ABCB1 substrate, it is likely that a similar process applies in our mouse models: inhibition of intestinal ABCB1 by the high concentration of oral rifampin results in reduced direct intestinal excretion and increased net absorption of larotrectinib, thus explaining the strongly reduced SI + SIC levels of larotrectinib upon rifampin treatment. Comparison of the rifampin SI + SIC data as larotrectinib percentage of dose in wild-type mice (5.2 %) with those obtained with elacridar treatment (2.0 %) show that elacridar is still a more effective inhibitor of intestinal ABCB1. The absence of clear shifts in brain- or other tissue distribution (apart from liver and SI + SIC) of larotrectinib suggests that, for instance, ABCB1 in the BBB was not markedly inhibited upon oral rifampin treatment (Supplemental Figures 4 and 5), presumably due to lower systemic concentrations of rifampin. Overall, the data suggest that in mice oral rifampin does not only inhibit hepatic Oatp1a/1b proteins, but also intestinal ABCB1 activity to some extent.

As FDA guidelines [5] indicate, coadministration of a strong CYP3A inhibitor (itraconazole) with a single 100 mg dose of larotrectinib in humans could increase the larotrectinib plasma AUC<sub>0-∞</sub> by 4.3-fold and the C<sub>max</sub> by 2.8-fold as compared to larotrectinib administered alone. Ritonavir, another strong CYP3A inhibitor, could profoundly enhance both paclitaxel and docetaxel oral availability in mice [22]. In the current study, given the prominent role of CYP3A in the pharmacokinetics of larotrectinib, the influence of oral ritonavir on oral larotrectinib pharmacokinetics was investigated. Again, to aim for complete inhibition of intestinal and hepatic Cyp3a and CYP3A4, a dose of 50 mg/kg oral ritonavir was used 15 min before larotrectinib administration. After pre-treatment with ritonavir, wild-type and Cyp3aXAV mice showed increased plasma exposure of larotrectinib to a similar level as seen in vehicle-treated Cyp3a<sup>-/-</sup> mice. Interestingly, ritonavir also enhanced the overall exposure of larotrectinib in Cyp3a<sup>-/-</sup> mice, suggesting additional effects of ritonavir on non-Cyp3a larotrectinib clearance mechanisms. While ritonavir primarily inhibits CYP3A-mediated metabolism, it is known that it can also inhibit ABCB1 [24,25]. As the results showed that ritonavir strongly reduced both liver and SI + SIC distribution of larotrectinib even in Cyp3a<sup>-/-</sup> mice, the most likely explanation is that ritonavir could also inhibit ABCB1 in both small intestine and liver, thus enhancing the larotrectinib exposure even when Cyp3a is absent. These results could not be logically explained by reduced metabolism of larotrectinib, for instance if ritonavir would inhibit another non-Cyp3a larotrectinib-metabolizing enzyme, as one would then expect relative increases in tissue levels of larotrectinib.

Strikingly, the relative effect of ritonavir on liver- and SI + SIC-to-plasma ratios was highest in the Cyp3a<sup>-/-</sup> mice, and lowest in the Cyp3aXAV mice (Supplemental Figure 7B, D, F). This suggests that ritonavir-mediated inhibition of Abcb1a/1b was strongest in the

Cyp3a<sup>-/-</sup> mice, lowest in the Cyp3aXAV mice, with the wild-type mice in between. This could in part relate to relative ritonavir exposure in liver and intestine of these strains. As ritonavir itself is also metabolized by and/or irreversibly bound to mouse and human CYP3A, the amount of available ritonavir in these organs may well be highest in the Cyp3a<sup>-/-</sup> mice, and lowest in the Cyp3aXAV mice. In contrast to its intestinal and hepatic disposition, the brain penetration of larotrectinib was not influenced by ritonavir. Like for rifampin, it may well be that the effective plasma concentration of ritonavir was too low to achieve noticeable inhibition of the ABC transporters in the BBB.

The combined activity of drug transporters and CYP3A results in efficient first-pass metabolism of orally administered drugs, and this phenomenon was also observed for many other drugs [11–15,23,37]. Considering that ritonavir inhibits both Cyp3a and ABCB1 proteins, it is difficult to conclude which inhibition function predominates for the increase of larotrectinib exposure in ritonavir-treated wild-type mice, but it seems likely that inhibition of ABCB1 by ritonavir does contribute to the increased oral bioavailability of larotrectinib.

Unlike some other drugs that are primarily affected by one or a few of the main detoxification systems, larotrectinib pharmacokinetics behavior can be affected by multiple factors, including but perhaps not limited to ABC transporters, OATP1A, and CYP3A. On the one hand, these properties may make it more likely that larotrectinib is affected by drug-drug interactions or genetic polymorphisms, thus possibly influencing its safety and efficacy profiles. On the other hand, being handled by multiple detoxification systems may make it less likely that one system will be very dominant, and have a disproportionate impact of larotrectinib pharmacokinetics. It is worth noting that the high dosages of the inhibitors used (especially for ritonavir and rifampin) may have contributed to the additional inhibitory effects, likely through the ABCB1 transporter(s), that were observed in the current study. Still, the fact that some known possibly co-administered drugs such as rifampin and ritonavir can simultaneously affect larotrectinib through multiple detoxification systems does pose a potential risk that needs to be carefully considered. Even though no signs of spontaneous toxicity of larotrectinib showed up in any of the tested mouse strains in the current experiments, given the complications observed, any attempt to apply “specific” inhibitors or combination therapy regimes in patients together with larotrectinib should be carefully monitored.

In summary, this study confirmed that larotrectinib is a substrate of mouse Oatp1a/1b, but not of human OATP1B1 and -1B3 *in vivo*. To the best of our knowledge, this is the first study documenting that elacridar could enhance larotrectinib plasma exposure as well as brain penetration. It was further found that rifampin can increase larotrectinib systemic exposure, most likely by inhibiting OATP1A, as well as by acute inhibition of enterocyte ABCB1. Similarly, ritonavir can also increase larotrectinib oral availability and thus its tissue exposure by inhibition of not only CYP3A enzymes, but also ABCB1 transporters in both small intestine and liver. The obtained drug-drug interaction insights and principles in this study may potentially be used to further optimize the therapeutic application and efficacy of larotrectinib in the clinic.

## Declaration of Competing Interest

The authors declare that they have no known competing financial interests or personal relationships that could have appeared to influence the work reported in this paper.

## Acknowledgements

This work was funded in part by the Chinese Scholarship Council (CSC Scholarship No. 201506240107 to Yaogeng Wang).

## Author contributions

Yaogeng Wang and Alfred H. Schinkel designed the study, analyzed

the data and wrote the manuscript. Yaogeng Wang, Rolf W. Sparidans, Jing Wang and Wenlong Li performed the experimental parts of the study. Maria C. Lebre contributed reagents, materials and mice, and checked the content and language of the manuscript. Jos H. Beijnen and Rolf W. Sparidans supervised the bioanalytical part of the studies and checked the content and language of manuscript. All authors commented on and approved the manuscript.

## Appendix A. Supplementary material

Supplementary data to this article can be found online at <https://doi.org/10.1016/j.ejpb.2021.12.007>.

## References

- [1] A. Nakagawara, Trk receptor tyrosine kinases: a bridge between cancer and neural development, *Cancer Lett.* 169 (2) (2001) 107–114.
- [2] L. Créancier, I. Vandenbergh, B. Gomes, C. Dejean, J.-C. Blanchet, J. Meilleroux, R. Guimbaud, J. Selves, A. Kruczyński, Chromosomal rearrangements involving the NTRK1 gene in colorectal carcinoma, *Cancer Lett.* 365 (1) (2015) 107–111.
- [3] G. Wu, et al., The genomic landscape of diffuse intrinsic pontine glioma and pediatric non-brainstem high-grade glioma, *Nat. Genet.* 46 (2014) 444–450.
- [4] N. Stransky, E. Cerami, S. Schalm, J.L. Kim, C. Lengauer, The landscape of kinase fusions in cancer, *Nat. Commun.* 5 (2014) 4846.
- [5] Food and Drug Administration. Center for Drug Evaluation and Research of the US Department of Health and Human Service, Food and Drug Administration. Multi-discipline Review (2018). Available from: [https://www.accessdata.fda.gov/drugsatfda\\_docs/label/2018/211710s0001b1.pdf](https://www.accessdata.fda.gov/drugsatfda_docs/label/2018/211710s0001b1.pdf).
- [6] A.H. Schinkel, J.W. Jonker, Mammalian drug efflux transporters of the ATP binding cassette (ABC) family: an overview, *Adv. Drug Deliv. Rev.* 55 (1) (2003) 3–29.
- [7] Y. Wang, R.W. Sparidans, W. Li, M.C. Lebre, J.H. Beijnen, A.H. Schinkel, OATP1A/1B, CYP3A, ABCB1, and ABCG2 limit oral availability of the NTRK inhibitor larotrectinib, while ABCB1 and ABCG2 also restrict its brain accumulation, *Br. J. Pharmacol.* 177 (13) (2020) 3060–3074.
- [8] A.-J. de Graan, C.S. Lancaster, A. Obaidat, B. Hagenbuch, L. Elens, L.E. Friberg, P. de Bruijn, S. Hu, A.A. Gibson, G.H. Bruun, T.J. Corydon, T.S. Mikkelsen, A. L. Walker, G. Du, W.J. Loos, R.H.N. van Schaik, S.D. Baker, R.H.J. Mathijssen, A. Sparreboom, Influence of polymorphic OATP1B-type carriers on the disposition of docetaxel, *Clin. Cancer Res. Off. J. American Assoc. Cancer Res.* 18 (16) (2012) 4433–4440.
- [9] A.E. van Herwaarden, E. Wagenaar, C.M.M. van der Kruijsen, R.A.B. van Waterschoot, J.W. Smit, J.-Y. Song, M.A. van der Valk, O. van Tellingen, J.W. A. van der Hoorn, H. Rosing, J.H. Beijnen, A.H. Schinkel, Knockout of cytochrome P450 3A yields new mouse models for understanding xenobiotic metabolism, *J. Clin. Investig.* 117 (11) (2007) 3583–3592.
- [10] F.P. Guengerich, Cytochrome P-450 3A4: regulation and role in drug metabolism, *Annu. Rev. Pharmacol. Toxicol.* 39 (1) (1999) 1–17.
- [11] L.X. Garmire, C.A. Hunt, In silico methods for unraveling the mechanistic complexities of intestinal absorption: metabolism-efflux transport interactions, *Drug Metabol. Disposit. Biolog. Fate Chem.* 36 (7) (2008) 1414–1424.
- [12] K.T. Kivistö, M. Niemi, M.F. Fromm, Functional interaction of intestinal CYP3A4 and P-glycoprotein, *Fundam. Clin. Pharmacol.* 18 (6) (2004) 621–626.
- [13] C. Wandel, et al., P-glycoprotein and cytochrome P-450 3A inhibition: dissociation of inhibitory potencies, *Cancer Res.* 59 (1999) 3944–3948.
- [14] K. Ito, H. Kusuura, Y. Sugiyama, Effects of intestinal CYP3A4 and P-glycoprotein on oral drug absorption—theoretical approach, *Pharm. Res.* 16 (1999) 225–231.
- [15] P. Watkins, The barrier function of CYP3A4 and P-glycoprotein in the small bowel, *Adv. Drug Deliv. Rev.* 27 (2–3) (1997) 161–170.
- [16] A. Martínez-Chávez, S. van Hoppe, H. Rosing, M.C. Lebre, M. Tibben, J.H. Beijnen, A.H. Schinkel, P-glycoprotein Limits Ribociclib Brain Exposure and CYP3A4 Restricts Its Oral Bioavailability, *Mol. Pharm.* 16 (9) (2019) 3842–3852.
- [17] S. Durmus, R.W. Sparidans, E. Wagenaar, J.H. Beijnen, A.H. Schinkel, Oral availability and brain penetration of the B-RAFV600E inhibitor vemurafenib can be enhanced by the P-GLYCOPROTEIN (ABCB1) and breast cancer resistance protein (ABCG2) inhibitor elacridar, *Mol. Pharm.* 9 (11) (2012) 3236–3245.
- [18] J.S. Lagas, R.A.B. van Waterschoot, R.W. Sparidans, E. Wagenaar, J.H. Beijnen, A. H. Schinkel, Breast cancer resistance protein and P-glycoprotein limit sorafenib brain accumulation, *Mol. Cancer Ther.* 9 (2) (2010) 319–326.
- [19] H. Kodaira, H. Kusuura, J. Ushiki, E. Fuse, Y. Sugiyama, Kinetic analysis of the cooperation of P-glycoprotein (P-gp/Abcb1) and breast cancer resistance protein (Bcrp/Abcg2) in limiting the brain and testis penetration of erlotinib, flavopiridol, and mitoxantrone, *J. Pharmacol. Experim. Therapeut.* 333 (3) (2010) 788–796.
- [20] L. Salphati, X. Chu, L. Chen, B. Prasad, S. Dallas, R. Evers, D. Mamaril-Fishman, E. G. Geier, J. Kehler, J. Kunta, M. Mezler, L. Laplanche, J. Pang, A. Rode, M.G. Soars, J.D. Unadkat, R.A.B. van Waterschoot, J. Yabut, A.H. Schinkel, N. Scheer, Evaluation of organic anion transporting polypeptide 1B1 and 1B3 humanized mice as a translational model to study the pharmacokinetics of statins, *Drug Metabol. Disposit. Biolog. Fate Chem.* 42 (8) (2014) 1301–1313.
- [21] M.L. Reitman, X. Chu, X. Cai, J. Yabut, R. Venkatasubramanian, S. Zajic, J.A. Stone, Y. Ding, R. Witter, C. Gibson, K. Roupe, R. Evers, J.A. Wagner, A. Stoch, Rifampin's acute inhibitory and chronic inductive drug interactions: experimental and model-based approaches to drug-drug interaction trial design, *Clin. Pharmacol. Ther.* 89 (2) (2011) 234–242.
- [22] J.J.M.A. Hendriks, J.S. Lagas, E. Wagenaar, H. Rosing, J.H.M. Schellens, J. H. Beijnen, A.H. Schinkel, Oral co-administration of elacridar and ritonavir enhances plasma levels of oral paclitaxel and docetaxel without affecting relative brain accumulation, *Br. J. Cancer* 110 (11) (2014) 2669–2676.
- [23] R. ter Heine, R.A.B. Van Waterschoot, R.J. Keizer, J.H. Beijnen, A.H. Schinkel, A.D. R. Huitema, An integrated pharmacokinetic model for the influence of CYP3A4 expression on the in vivo disposition of lopinavir and its modulation by ritonavir, *J. Pharm. Sci.* 100 (6) (2011) 2508–2515.
- [24] H. Gutmann, G. Fricker, J. Drewe, M. Toeroek, D.S. Miller, Interactions of HIV protease inhibitors with ATP-dependent drug export proteins, *Mol. Pharmacol.* 56 (2) (1999) 383–389.
- [25] J. Drewe, H. Gutmann, G. Fricker, M. Török, C. Beglinger, J. Huwyler, HIV protease inhibitor ritonavir: a more potent inhibitor of P-glycoprotein than the cyclosporine analog SDZ PSC 833, *Biochem. Pharmacol.* 57 (10) (1999) 1147–1152.
- [26] R.W. Sparidans, Y. Wang, A.H. Schinkel, J.H.M. Schellens, J.H. Beijnen, Quantitative bioanalytical assay for the tropomyosin receptor kinase inhibitor larotrectinib in mouse plasma and tissue homogenates using liquid chromatography-tandem mass spectrometry, *J. Chromatogr. B* 1102–1103 (2018) 167–172.
- [27] J.W. Jonker, J. Freeman, E. Bolscher, S. Musters, A.J. Alvi, I. Titley, A.H. Schinkel, T.C. Dale, Contribution of the ABC transporters Bcrp1 and Mdr1a/1b to the side population phenotype in mammary gland and bone marrow of mice, *Stem Cells* 23 (8) (2005) 1059–1065.
- [28] E. van de Steeg, et al., Organic anion transporting polypeptide 1a/1b-knockout mice provide insights into hepatic handling of bilirubin, bile acids, and drugs, *J. Clin. Investig.* 120 (2010) 2942–2952.
- [29] E. van de Steeg, C.M.M. van der Kruijsen, E. Wagenaar, J.E.C. Burggraaf, E. Mesman, K.E. Kenworthy, A.H. Schinkel, Methotrexate pharmacokinetics in transgenic mice with liver-specific expression of human organic anion-transporting polypeptide 1B1 (SLCO1B1), *Drug Metabol. Disposit. Biolog. Fate Chem.* 37 (2) (2009) 277–281.
- [30] E. van de Steeg, A. van Esch, E. Wagenaar, K.E. Kenworthy, A.H. Schinkel, Influence of human OATP1B1, OATP1B3, and OATP1A2 on the pharmacokinetics of methotrexate and paclitaxel in humanized transgenic mice, *Clin. Cancer Res. Off. J. American Assoc. Cancer Res.* 19 (4) (2013) 821–832.
- [31] Y. Zhang, M. Huo, J. Zhou, S. Xie, PKSolver: An add-in program for pharmacokinetic and pharmacodynamic data analysis in Microsoft Excel, *Comput. Methods Programs Biomed.* 99 (3) (2010) 306–314.
- [32] R. Sane, S. Agarwal, W.F. Elmquist, Brain distribution and bioavailability of elacridar after different routes of administration in the mouse, *Drug Metabol. Disposit. Biolog. Fate Chem.* 40 (8) (2012) 1612–1619.
- [33] W. Li, R.W. Sparidans, Y. Wang, M.C. Lebre, E. Wagenaar, J.H. Beijnen, A. H. Schinkel, P-glycoprotein (MDR1/ABCB1) restricts brain accumulation and cytochrome P450-3A (CYP3A) limits oral availability of the novel ALK/ROS1 inhibitor lorlatinib, *Int. J. Cancer* 143 (8) (2018) 2029–2038.
- [34] W. Li, R.W. Sparidans, Y. Wang, M.C. Lebre, J.H. Beijnen, A.H. Schinkel, P-glycoprotein and breast cancer resistance protein restrict brigatinib brain accumulation and toxicity, and alongside CYP3A, limit its oral availability, *Pharmacol. Res.* 137 (2018) 47–55.
- [35] J. Wang, M.A.C. Bruin, C. Gan, M.C. Lebre, H. Rosing, J.H. Beijnen, A.H. Schinkel, Brain accumulation of tivozanib is restricted by ABCB1 (P-glycoprotein) and ABCG2 (breast cancer resistance protein) in mice, *Int. J. Pharm.* 581 (2020) 119277, <https://doi.org/10.1016/j.ijpharm.2020.119277>.
- [36] B. Greiner, M. Eichelbaum, P. Fritz, H.-P. Kreichgauer, O. von Richter, J. Zundler, H.K. Kroemer, The role of intestinal P-glycoprotein in the interaction of digoxin and rifampin, *J. Clin. Investig.* 104 (2) (1999) 147–153.
- [37] L.Z. Benet, C.L. Cummins, The drug efflux-metabolism alliance: biochemical aspects, *Adv. Drug Deliv. Rev.* 50 (Suppl 1) (2001) S3–S11.